International Journal of Pharmaceutics 378 (2009) 23–29

Contents lists available at ScienceDirect

International Journal of Pharmaceutics

journal homepage: www.elsevier.com/locate/ijpharm

An innovative floating gastro retentive dosage system: Formulation and in vitro evaluation

C. Sauzet [a,b], M. Claeys-Bruno [b], M. Nicolas [c], J. Kister [b], P. Piccerelle [a], P. Prinderre [a,*]

[a] Université de la Méditerranée, EA 4263, Faculté de Pharmacie, Marseille Laboratoire de Pharmacie galénique, 27, Boulevard Jean Moulin, 13385 Marseille Cedex 5, France
[b] Université Paul Cézanne, ISM2 UMR6263 ADDEM, laboratoire des Systèmes chimiques complexes, Faculté des sciences et techniques de Saint Jérôme Service, 451 Avenue Escadrille Normandie-Niémen, 13397 Marseille Cedex 20, France
[c] Université de Provence, UMR 6595 IUSTI l'Ecole Polytechnique Universitaire de Marseille, 5 rue Enrico Fermi, 13543 Marseille Cedex 13, France

ARTICLE INFO

Article history:
Received 9 March 2009
Received in revised form 12 May 2009
Accepted 16 May 2009
Available online 22 May 2009

Keywords:
Floating tablet
Gastro retentive dosage form
Experimental design
Hydrophobic dusty powder
Wet granulation

ABSTRACT

Over the years, different formulation technologies intended for gastro retentive dosage delivery were investigated and patented. The aim of this study was to develop an innovative floating gastro retentive dosage form (GRDF). The developed technology induces a low-density dosage form containing high active pharmaceutical ingredient (API) concentration by using a hydrophobic dusty powder excipient under specific conditions. The new dosage form was obtained by state of the art wet granulation manufacturing process. An experimental design using a discrete variable and four mixture variables was conducted in order to optimize API concentration and buoyancy of the new dosage form. An apparatus was developed to measure the apparent density of floating tablet. The GRDF was characterized for apparent density, buoyancy, porosity and dissolution using in vitro experimentations.

© 2009 Elsevier B.V. All rights reserved.

1. Introduction

Oral delivery of drugs is the most preferred administration route due to ease of administration. Drug bioavailability of pharmaceutical oral dosage forms is influenced by various factors. One important factor is the gastric residence time (GRT) of these dosage forms (Kagan and Hoffman, 2008; Desai and Bolton, 1993). Indeed, gastric retention has received significant interest in the past few decades as most of the conventional oral delivery systems have shown some limitations related to fast gastric emptying time. A gastro retentive dosage form (GRDF) can overcome this problem and is particularly useful for drugs that are primarily absorbed in the duodenum and upper jejunum segments. The classification of different modes of gastric retention has been listed by Hwang et al. (1998) and Bardonnet et al. (2006):

- high-density (sinking) systems,
- low-density (floating) systems,
- expandable systems,
- superporous hydrogel systems,
- mucoadhesive systems
- and magnetic systems.

The stomach is divided into 3 anatomic regions: fundus, body, and antrum (pylorus). The separation between stomach and duodenum is the pylorus. The part made of fundus and body acts as a reservoir for undigested material, whereas the antrum is the main site for mixing motions and act as a pump for gastric emptying by propelling actions. Gastric emptying occurs during fasting as well as fed states. The pattern of motility is however distinct for the two states. During the fasting state an interdigestive series of electrical events take place, which cycle both through stomach and intestine every 2–3 h. This is called the interdigestive myloelectric cycle or migrating myloelectric cycle (MMC), which is further divided into following 4 phases as described by Struebel et al. (2006):

- Phase I (basal phase) lasts from 40 to 60 min with rare contractions.
- Phase II (preburst phase) lasts from 40 to 60 min with intermittent action potential and contractions. As the phase progresses the intensity and frequency also increases gradually.
- Phase III (burst phase) lasts for 4–6 min. It includes intense and regular contractions for short period. It is due to this wave that all the undigested material is swept out of the stomach down to the small intestine. It is also known as the housekeeper wave.

* Corresponding author. Tel.: +33 4 91 83 56 69; fax: +33 4 91 83 78 75 75.
E-mail address: pprinderre@pharmacie.univ-mrs.fr (P. Prinderre).

0378-5173/$ – see front matter © 2009 Elsevier B.V. All rights reserved.
doi:10.1016/j.ijpharm.2009.05.027

- Phase IV lasts for 0–5 min is a transition period of decreasing activity until the next cycle begins.

Food effects and the complex motility of the stomach play a major role in gastric retention behavior (Klausner et al., 2003; O'Reilly et al., 1987; Sangekar et al., 1987; Khosla et al., 1989; Abrahamsson et al., 1993). Several approaches of non-effervescent and effervescent formulation technologies have been used and patented in order to increase gastric residence time of the GRDF (Talwar et al., 2000; Sonobe and Watanabe, 1989; Berner and Hou Sui Yuen, 2004; Curatolo and Lo, 1988; Afargan et al., 2006; Vanderbist et al., 2007). Streubel et al. (2003a) prepared floating matrix tablets using a low-density polypropylene foam powder and matrix-forming polymers. They also developed microparticles based on low-density foam powder (Streubel et al., 2002, 2003b). The incorporation of low-density materials, such as edible oils, in the dosage forms has been also reported recently. Fukuda et al. (2006) investigated floating hot-melt extruded tablets for gastroretentive controlled drug release system.

Floating characteristic of a gastric retentive dosage form is assessed by onset of floating, floating duration but also floating strength. The floating strength has not been quantified extensively in previous studies. However, it represents an important characteristic as the dosage form has to float *in vivo* even in the presence of food. As higher floating strength increases the probability of the oral dosage form to remain afloat, this attribute plays a major role in reducing food effects on gastric retention.

The objective of the present work was to develop a new and innovative gastroretentive formulation based on intrinsic low-density (floating) systems using a standard manufacturing process (the wet granulation and the moulding of the tablets have been chosen), allowing a final porous structure with improved cohesion and which releases drugs in the stomach and upper gastrointestinal (GI) tract. The floating system must have an intrinsic density lower than 1.004 g/cm^3. In our technology, the buoyancy is provided first by a high porosity, and secondly by the high content of hydrophobic compounds. In order to enhance the final tablet porosity, a high shear mixer was used during the wet granulation process to incorporate some air into the produced paste. The roles of each compound and each parameter on buoyancy were characterized through an experimental design. With this experimental design the critical process parameters have been frozen to compare the results. The responses which have been studied were the apparent density and the porosity of tablets issued from our manufacturing process. The experimental design induced 28 runs, but dissolution profiles have been achieved only on 4 specific runs.

2. Materials and methods

2.1. Materials

Theophyllinee was used as model drug (COOPER, France). Silicon Dioxyde (Aerosil® R972, Degussa, Germany) was used as a hydrophobic dusty powder. Polyvinilpyrollidone/PVP K30 (Kollidon® 30, BASF, Germany) was used as a binder. Stearic acid was used as controlled release agent (COOPER, France). All other chemicals used were of reagent grade.

2.2. GRDF manufacturing process

Aqueous wet granulation and moulding processes have been chosen as state of the art pharmaceutical manufacturing processes for the GRDF formulations. In order to enhance the final tablet porosity a high shear granulator (4M8-Granulator high shear granulator and pelletizer, Pro-C-epT®, Belgium) was used to incorporate air into the produced wet mass. The following procedure was applied for wet granulation of the different formulations listed in Table 1.

All the runs were achieved without chopper:

- Raw material weighing.
- Dry mixing with impeller at 150 rpm for 150 s.

Table 1
Parameters of experimental runs with the responses (2 last columns).

Run	X_1 Oven T° (°C)	X_2 API %	X_3 Stearic acid %	X_4 Povidone K30 %	X_5 Aerosil R972 %	Y_1 Apparent density (kg/m^3)	Y_2 Porosity
1	40	85.00	5.00	5.00	5.00	1300.75	0.08
2	40	70.00	5.00	20.00	5.00	1110.63	0.21
3	40	55.00	20.00	20.00	5.00	1071.01	0.18
4	40	70.00	5.00	5.00	20.00	746.67	0.48
5	40	55.00	5.00	20.00	20.00	1057.74	0.28
6	40	50.00	20.00	10.00	20.00	651.90	0.53
7	40	77.50	12.50	5.00	5.00	1191.05	0.12
8	40	62.50	20.00	5.00	12.50	719.08	0.48
9	40	61.00	13.00	13.00	13.00	1037.04	0.26
10	60	85.00	5.00	5.00	5.00	1254.58	0.10
11	60	70.00	20.00	5.00	5.00	1082.86	0.20
12	60	55.00	20.00	5.00	20.00	620.54	0.55
12'	60	55.00	20.00	5.00	20.00	590.66	0.57
12"	60	55.00	20.00	5.00	20.00	628.28	0.55
13	60	50.00	10.00	20.00	20.00	776.75	0.45
14	60	50.00	20.00	20.00	10.00	892.49	0.23
15	60	77.50	5.00	12.50	5.00	1144.56	0.21
16	60	77.50	5.00	5.00	12.50	1019.18	0.32
17	60	62.50	20.00	12.50	5.00	879.83	0.35
18	60	62.50	12.50	20.00	5.00	1177.40	0.16
19	60	62.50	5.00	20.00	12.50	1197.36	0.16
20	60	62.50	12.50	5.00	20.00	631.61	0.57
21	60	62.50	5.00	12.50	20.00	809.46	0.46
22	60	52.50	18.60	10.30	18.60	665.87	0.52
23	60	65.50	9.00	16.50	9.00	1217.58	0.15
24	40	65.50	9.00	9.00	16.50	780.33	0.44
25	40	58.00	16.50	9.00	16.50	738.62	0.47
D	60	57.00	19.00	5.00	19.00	574.21	0.58

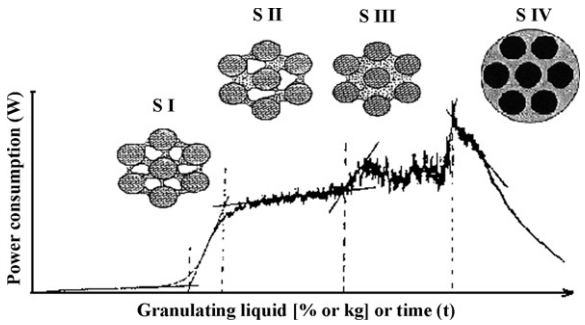

Fig. 1. Schematisation of wet granulation steps using measurement of impeller torque in function of quantity of granulating liquid (SI: pendular step, SII: funicular step, SIII: capillary step, and SIV: droplets step).

- Granulation at 10 ml/min with impeller at 1000 rpm for 8 min.
- Final mixing with impeller at 1500 rpm for 60 s.

Torque variations were recorded throughout granulation process. Tablets were then made by moulding the wet mass into PVC cavity with a diameter of 13.5 mm and a thickness of 7.1 mm. The mass was then dried in a ventilated oven (MMM® venticell type 404). Target loss on drying (HR < 3% for each run) was measured at 120 °C for 10 min using an infrared balance (Precisa® 310 M).

According to the data recorded, the granulation phenomenon is represented in Fig. 1, showing the formation of bridges between the solid particles with the increase of quantities of the granulating solution, the saturation which is reached once the interparticular void spaces have been filled up (step IV), and finally the over-granulated state with the solid system turning into liquid. Each step represents a progressive increase in the moisture content, agglomeration mechanism is a gradual change from a triphasic stage (air–liquid–solid) in which granules are in pendular (I) and funicular (II) states to a biphasic (liquid–solid) in which the granules are in the capillary (III) and droplets (IV) state. The granulating parameters are therefore closely controlled at any of the design and operation stages of the manufacturing process, to avoid that the material becomes irremediably lost as soon as it reaches the critical granulating point. Overgranulating is usually avoided in the pharmaceutical industry, but required for the developed GRDF process.

2.3. Determination of true and apparent density and floating strength of GRDF tablets

The true density of the GRDF was measured ($n = 10$) using a helium pycnometer (Accupyc 1330, Micrometrics). Floating strength of the developed systems was determined using an apparatus and methodology based on Timmermanns and Moës (Timmermans, 1991) (Timmermans and Moës, 1990a,b,c).

The apparent density of the tablets ρ_a was determined using a custom apparatus, based on an immersed beam measuring the buoyancy force. The apparatus was made of a transparent parallelepipedic box filled with a liquid with a known density, which is simulated gastric dissolution media HCl 0.1N pH 1.2 (European Pharmacopoeia 6.0). A thin flexible PMMA beam (thickness $h = 1$ mm thick, $w = 20$ mm wide and $L = 25$ cm long) was immersed in the bath and was equipped with a sample holder made with metal wires (see Fig. 2) at its free extremity. The other extremity was held firmly.

When the solid dosage was placed into the sample holder, it was vertically displaced by the buoyancy force and reached a new steady state once the beam oscillations vanished. Measurement of the induced deviation ($n = 6$) in two dimensions allows the calculation of its density according to the Eq. (3) obtained by combination

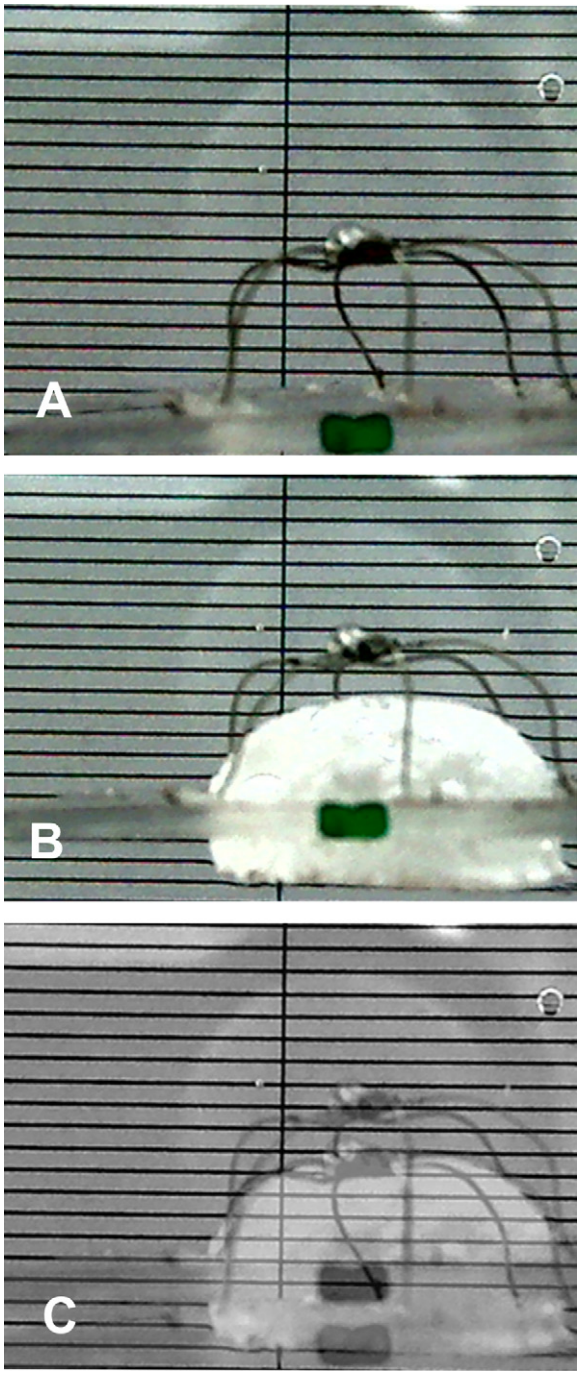

Fig. 2. Experimental setup for the determination of the apparent density A: image of the beam extremity with the sample holder. B: Due to the buoyant force of the tablet, the beam is lifted vertically. C: Difference between photographs A and B showing the displacement δ_c. The millimetre scale is seen in the back.

of the following Eqs. (1) and (2). According to Archimedes's principle, the vectorial sum of the gravity (F_{grav}) and buoyancy (F_{buoy}) forces acting on the tablet determines the magnitude and direction of force F and thus the resultant weight of the floating object:

$$F = F_{buoy} - F_{grav}$$
$$F = \rho_f g V - \rho_a g V = (\rho_f - \rho_a) g V \quad (1)$$

where F is the total vertical force, g the acceleration of gravity, and V the tablet volume.

The determination of displacement induced by the tablet is given by:

$$\delta_c = 4\frac{L^3}{Ewh^3}F \quad (2)$$

where F is the force acting on the free extremity of the beam combining Eqs. (1) and (2) gives a direct expression for the tablet apparent density:

$$\rho_a = \frac{\rho_f}{1 - Ewh^3\delta_c/4gL^3m_c} \quad (3)$$

where ρ_f is the liquid density, m_c is the tablet weight, δc is the displacement of the beam and E is the elastic modulus of beam material (Young's modulus).

The beam displacement δ_c was measured by comparing two digital photographs captured with a webcam (QuickCam® Pro 9000 Logitech, resolution 1600 × 1200 pixels) before and after the tablet insertion into the sample holder. The ImageJ software (http://rsbweb.nih.gov/ij/) allowed us to superpose the two images, to calibrate the images and to compute the displacement (Fig. 2). A millimetre scale was placed on the back wall of the tank for image calibration. According to these specifications, the accuracy of this apparatus was 10^{-5} N on the buoyancy force. A standard mass with a known volume was used as internal standard.

2.4. Calculation of tablet porosity

True and apparent density values of the GRDF are required for eestimation of the porosity (experimental design response). The porosity ε of the samples was then calculated:

$$\varepsilon = 1 - \frac{\rho_a}{\rho_t} \quad (4)$$

ρ_a represents the apparent density and ρ_t the true density of the samples. Porosity was also visually assessed by scanning electron microscopy of the tablets showing the lowest and highest porosity.

2.5. Experimental design

In order to evaluate the impact of formulation and process parameters on the buoyancy of the GRDF, an experimental design (NemrodW® software (Mathieu et al., 1999)) has been conducted. The responses which have been studied were the apparent density and the porosity of tablets issued from formulations and processes. The present study considered one quantitative variable and four mixture variables within the following experimental range:

Quantitative variable

X_1: Oven temperature: 40 or 60 °C.

Mixtures variables:

X_2: % of API: 50–85%.
X_3: % of stearic acid: 5–20%.
X_4: % PVP K30: 5–20%.
X_5: % of Aerosil R972: 5–20%

2.5.1. Mathematical modeling

An empirical mathematical model, based on five predictor variables, was built as follows and applied on selected runs as described in Section 2.5.2.

The quantitative variable is described with a first degree model using X_1 to represent the non-dimensional coded variable:

$$\eta_q = \beta_0 + \beta_1 X_1 \quad (5)$$

The four mixture variables (X_2, X_3, X_4, X_5) are described with a reduced cubic model in the component fraction X_i, for the defined domain:

$$\eta_m = \beta_2X_2 + \beta_3X_3 + \beta_4X_4 + \beta_5X_5 + \beta_{23}X_2X_3 + \beta_{24}X_2X_4 + \beta_{25}X_2X_5 + \beta_{34}X_3X_4 + \beta_{35}X_3X_5 + \beta_{45}X_4X_5 + \beta_{234}X_2X_3X_4 + \beta_{235}X_2X_3X_5 + \beta_{245}X_2X_4X_5 + \beta_{345}X_3X_4X_5 \quad (6)$$

Finally, the complete model describing the variation of the responses is additive (without interaction), $\eta_q + \eta_m$:

$$\eta = \eta_q + \eta_m = \beta_1X_1 + \beta_2X_2 + \beta_3X_3 + \beta_4X_4 + \beta_5X_5 + \beta_{23}X_2X_3 + \beta_{24}X_2X_4 + \beta_{25}X_2X_5 + \beta_{34}X_3X_4 + \beta_{35}X_3X_5 + \beta_{45}X_4X_5 + \beta_{234}X_2X_3X_4 + \beta_{235}X_2X_3X_5 + \beta_{245}X_2X_4X_5 + \beta_{345}X_3X_4X_5 \quad (7)$$

In order to estimate the coefficients of the mathematical model, runs were carefully chosen.

2.5.2. Choice of the experimental design

A "classical" design of experiments could not be used, because of the complexity of the experimental domain: firstly, the presence of quantitative variable and mixture variables and secondly, mixture variables with individual constraints.

To build the optimal design within the experimental domain for estimating the model coefficients, an exchange algorithms (Fedorov, 1972; Mitchell, 1974) has been used to extract a D-optimal design from a set of candidate points. At first, the experimental domain is covered with a set of possible experiments, namely candidate points, representing a good initial design for each model.

A grid design (Box and Wilson, 1951; Droesbeke and Montgomery, 1997) was built to study the quantitative variable: Temperature of the oven (X_1). For each two points of this grid design, a mixture design with 43 runs was built (Cornell, 1990; Scheffé, 1963) to obtain 86 candidate points. Using the exchange algorithm based on D-optimality criteria (Kiefer and Wolfowitz, 1959), 21 minimal experiments were finally selected that corresponded to a good quality design for the postulated model. In order to estimate the variance of the experimental error, the run no. 12 has been achieved in triplicate. Table 1 lists the experimental runs, the desirability run (run D) and the results of the two studied responses, apparent density (Y_1) and porosity (Y_2).

2.5.3. Desirability

Desirability function has been investigated in order to determine the optimized formulation. This tool is achieved by transforming the responses Y_i into a Di function called desirability function which is defined in a specific range of the variation of Y_i.

2.6. Controlled release studies

As the experimental design induced 28 runs, dissolution profiles have been achieved only on 4 specific runs. Dissolution profiles (over 9 h for the runs 1, 10, 12 and over 24 h for the run D) were performed using a USP apparatus II, paddle with sinkers. For this purpose an automatic dissolution tester (AT 7, Sotax, Switzerland) was used, operating with 1 l of 0.1N HCl (pH 1.2) at 37 ± 0.5 °C and paddle speed at 150 rpm to create sufficient vortex. Quantification of dissolved theophylline was determined by UV measurement at a wavelength of 271 nm.

3. Results and discussion

3.1. Manufacturing process

The developed process is based on the surprising finding that the resulting overgranulated materials, after that the granulating liquid was extracted to dryness, showed advantageous intrinsic low density and intrinsic high porosity that in fact serve in the manufacture of a floating sustained release dosage form. These advantageous characteristics resulted from the incorporation of air into the mass of the material via the overgranulation phenomena or indirectly through evaporation of entrapped water.

3.2. Experimental design

3.2.1. Study of apparent density

Coefficients of the mathematical model have been calculated from the experimental results. In order to validate the prediction model, four test points (22–25) have been studied to evaluate the experimental variance (Table 2).

Statistical tests on the residual values led to accept the following predictive model:

$$\begin{aligned} Y_1 = {} & -9.12X_1 + 1690.90X_2 - 15014.36X_3 + 17611.33X_4 \\ & -10346.50X_5 + 20045.21X_2X_3 - 27119.48X_2X_4 \\ & -10097.01X_2X_5 + 8629.89X_3X_4 + 119858.71X_3X_5 \\ & -64099.10X_4X_5 + 35391.55X_2X_3X_4 - 150650.48X_2X_3X_5 \\ & +145498.57X_2X_4X_5 - 128731.65X_3X_4X_5 \end{aligned} \quad (8)$$

The first finding is that the quantitative variable – oven temperature – did not impact on the apparent density response suggesting that the two tested temperatures are equivalent. The estimated effect of X_1 oven temperature (−9.12 cf Eq. (8)) is shown to be not statistically significant. Secondly, response surface are drawn within the experimental domain in the contour plot shown in Fig. 3. For clarity purposes, the percentage of PVP K30 (X_4) has been fixed to 10% in Fig. 3.

According to Fig. 3, the increase of API percentage (X_2) led to an increase of the density. The same phenomenon but less important was observed with the PVP K30 (X_4). It can also be seen that stearic acid (X_3) did not impact significantly the density. Moreover, an increase of Aerosil R972 percentage (X_5) had a strong influence on increasing the density.

3.2.2. Study of tablet porosity

Produced tablets are significantly different as per their porosity with variations ranging from 0.08 to 0.58 (cf Table 1). The porosity shows a strong linear correlation with the density (cf Eq. (4)) with a negative slope (Fig. 4). One can see that the porosity increases, when the density decreases.

This correlation implies the same behavior of the variables that means the same interpretation concerning the influence of the components in the formulation.

Porosity within the internal structure of GRDF was investigated using scanning electron microscopy on tablets which had the lowest and maximal response values. Tablets from run 1 (apparent density = 1300.75 kg/m^3 and porosity = 0.08) and run 12 (apparent density = 620.54 kg/m^3 and porosity = 0.55) have been cut according to their width and the pictures from the cross section are presented in Fig. 5. Higher porosity structure of run 12 that exhibits global monolithic aerated structure can be observed.

Table 2
Study of the residuals for the test points.

No. run	$Y_{exp.}$	$Y_{calc.}$	Difference
22	665.87	653.24	12.63
23	1217.58	1125.50	92.08
24	780.32	896.34	−116.02
25	738.62	764.83	−26.21

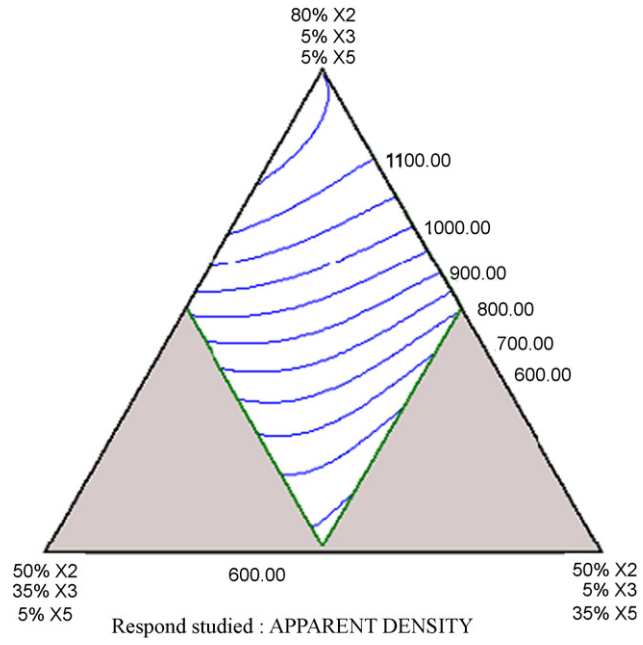

Fig. 3. Response variation in the experimental domain API (X_2), stearic acid (X_3), Aerosil R972 (X_5); fixed parameters: Povidone K30 (X_4) = 10%; T (°) oven (X_1) = 60 °C.

3.2.3. Desirability (Di)

In this study, in order to have a significant response, we have arbitrarily chosen the target (or minimal) value for density is 580 kg/m^3 and maximum accepted value is 800 kg/m^3. These values are inferior to gastric fluid density = 1004 kg/m^3.

This requirement is plotted in Fig. 6.

An algorithm is then applied in order to determine the set of variables that maximizes the Di function in order to minimize the density. Moreover, we imposed a constraint on the API percentage, which have to be >55%. From this required values (response and percentage), the optimum formula has been determined as Run D (Table 1), who represents the optimal conditions and allows the obtention of experimental response (apparent density) 574.21 kg/m^3 for a density predicted at 626.87 kg/m^3.

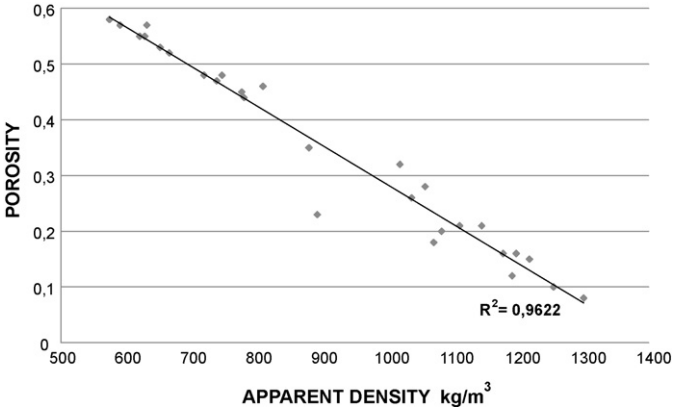

Fig. 4. Graphical representation of the correlation between porosity and apparent density.

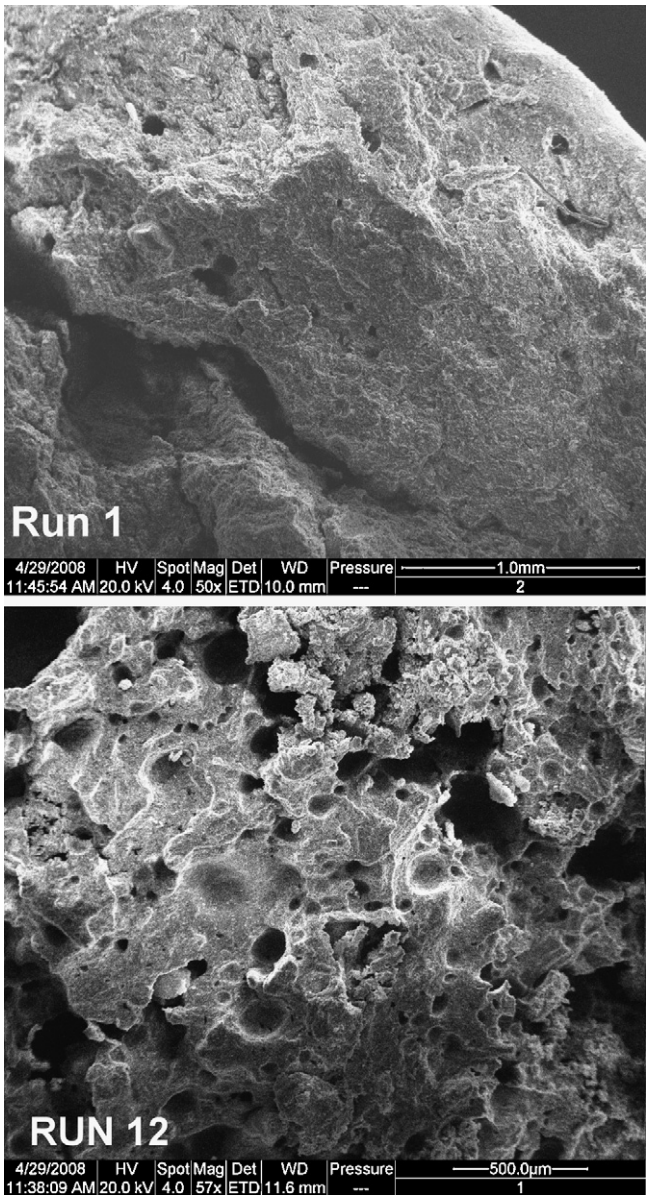

Fig. 5. Microphotograph on the left: cross section of tablets from run 1 (high density); microphotograph on the right: cross section of tablets from run 12 (low density).

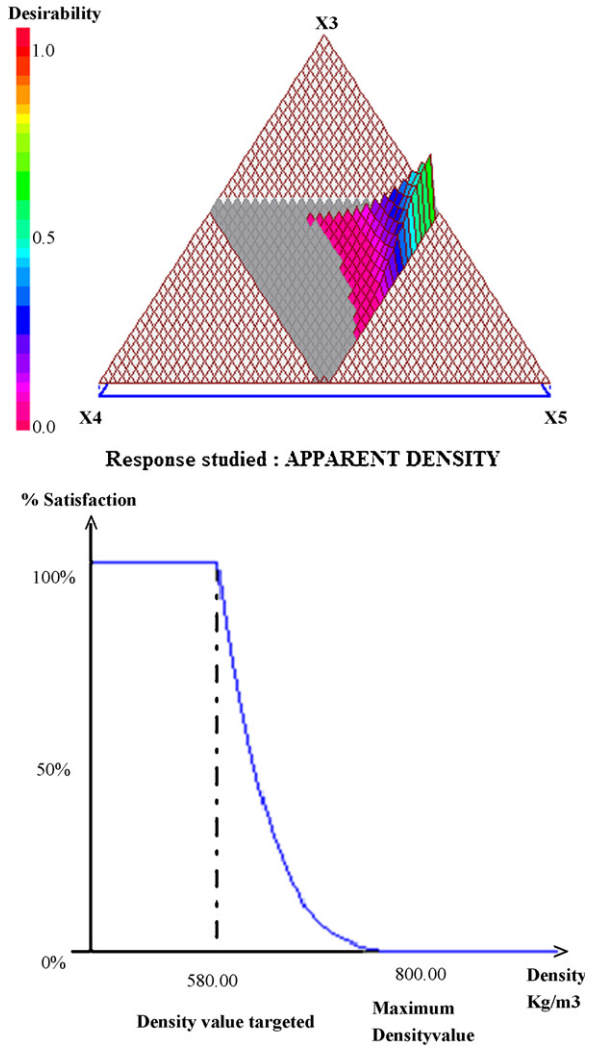

Fig. 6. Graphical representation 3D of desirability (A: API (X_2) rate is fixed at 55%, oven (X_1) is fixed at 60 °C, stearic acid (X_3), Aerosil R972 (X_5); Povidone K30 (X_4)) and variations of desirability function (B).

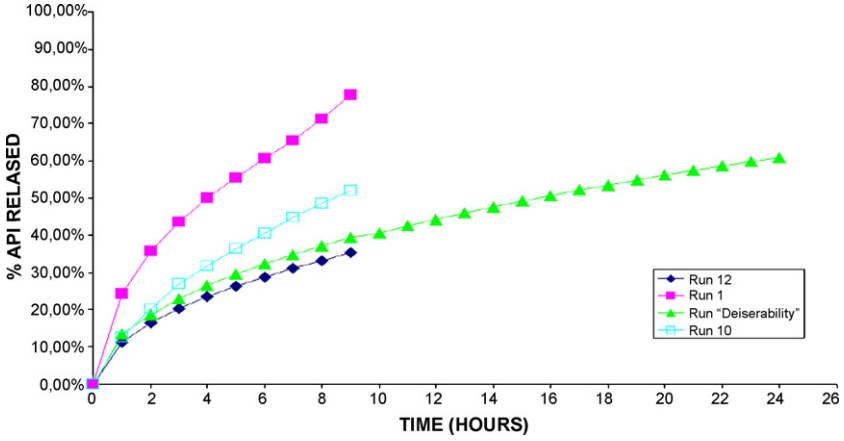

Fig. 7. Dissolution profiles of lower density tablet run 12 ♦, higher density tablet run 1 ■ run 10 □, and desirability tablet (run D) ▲ realized with the experimental design.

How one can see in Fig. 6, when the API rate is fixed at 55%, the lower apparent density is observed with high rates of stearic acid and Aerosil R972. The PVP K30 fixed at 5% is sufficient to remain the tablet structure integrity during a long time (up to 9 h) under dissolution test conditions (Fig. 7).

3.3. Controlled release studies based on experimental design runs

Four runs 1, 10, 12 and D from the experimental design (Table 1) were selected as they exhibit the extreme apparent density values. Even if run 1 and run 10 cannot be considered as GRDF, they were also studied in order to evaluate the impact of porosity and of oven temperature on dissolution profiles. Optimized formulation based on desirability calculation was investigated as well.

Dissolution profiles are presented in Fig. 7. Buoyancy of tablets was verified at the beginning and at the end of the dissolution test, Runs 12 and D still float at the end.

All formulations led to sustained release of theophylline. Although, high porosity tablets showed slower dissolution profiles, indeed run D exhibit an API release of about 50% after 24 h.

The sustained release cannot be only attributed to the porosity, as the tablets presenting higher porosity contain more hydrophobic ingredients. One can see that sustain release occurred even with only 5% percent of those ingredients. Comparison between profiles from run 1 and 10 exhibit that if the oven temperature has no effect on the tablet density, it has strong influence on the API release due to stearic acid low melting point (#55 °C).

Those results suggest that even with a high degree of air in the matrix, the cohesion of the monolithic structure is sufficient to sustain the release even under high agitation conditions (150 rpm for paddle speed rotation).

Finally, 5% of the binder was found to be sufficient to keep the tablet cohesion during a floating period of up to 9 h for run 12 and up to 24 h for run D.

4. Conclusion

This study has shown a proof of concept concerning an overgranulation manufacturing process of gastro retentive & sustain release platform using a hydrophobic dusty powder in order to obtain a wet aerates mass (Prinderre, 2008). The buoyancy of the developed technology is provided by two phenomenons: (1) high porosity of the dosage form and (2) high content of hydrophobic compounds.

Incorporation of silicon dioxide, commonly used as a glidant, allowed the production of a floating sustained release dosage form. According to the manufacturing process and to its hydrophobicity, the small particle size is allowing the reorganisation of the ingredient around the droplets of water. This water entrapment allows the obtention of pores during the drying step process with the water evaporation. Surprisingly, the high porosity of the matrix did not led to a weak structure which could be due to the presence of the binder.

In conclusion, the incorporation of a hydrophobic dusty powder using a classical wet granulation technique represent a new alternative for the obtention of sustain release dosage form and if the process undergo overgranulation, it represents an innovative formulation for a gastro retentive platform.

References

Abrahamsson, B., Alpsten, M., Hugosson, M., 1993. Absorption, gastrointestinal transit, and tablet erosion of felodipine extended-release (ER) tablets. Pharm. Res. 10, 709–714.

Afargan, M., Kirmayer, D., Lapidot, N., Friedman, M., Hoffman, A., 2006. Patent no. WO 2006072948.

Bardonnet, P., Faivre, V., Pugh, W., Piffaretti, J., Falson, F., 2006. Gastroretentive dosage forms: overview and special case of *Helicobacter pylori*. J. Control. Release 111, 1–18.

Berner, B., Hou Sui Yuen, E., 2004. US Patent no. 20040903879.

Box, G., Wilson, K., 1951. On the experimental attainment of optimum conditions. J. R. Stat. Soc. B 13, 1–45.

Cornell, J., 1990. Experiments with Mixtures: Designs, Models, and the Analysis of Mixture Data. Willey, New York.

Curatolo, W., Lo, J. 1988. US Patent no. 19880200801.

Desai, S., Bolton, S., 1993. A floating controlled-release drug delivery systems: in vitro–in vivo evaluation. Pharm. Res. 10, 1321–1325.

Droesbeke, J.F., Montgomery, D., 1997. Plans d'expériences: Applications à l'entreprise. Editions Technip.

Fedorov, V., 1972. Theory of Optimal Experiments. Academic Press, New York.

Fukuda, M., Peppas, N., McGinity, J., 2006. Floating hot-melt extruded tablets for gastroretentive controlled drug release system. J. Control. Release 115, 121–129.

Hwang, S.J., Park, H., Park, K., 1998. Gastric retentive drug-delivery systems. Ther. Drug Carrier Syst. 15, 243–284.

Kagan, L., Hoffman, A., 2008. Systems for region selective drug delivery in gastrointestinaltract: biopharmaceutical considerations. Expert Opin. Drug Deliv. 5, 681–692.

Khosla, R., Feely, L., Davis, S.G.-d., 1989. Int. J. Pharm. 53, 107–117.

Kiefer, J., Wolfowitz, J., 1959. Optimum designs in regression problems. Ann. Math. Stat. 30, 271–294.

Klausner, A., Eyal, S., Lavy, E., Friedman, M., Hoffman, A., 2003. Novel levodopa gastroretentive dosage form: in-vivo evaluation in dogs. J. Control. Release 88, 117–126.

Mathieu, D., Nony, J., Phan-Tan-Luu, R., 1999. NemrodW V2000. LPRAI, Marseille, France.

Mitchell, T., 1974. An algorithm for the construction of D-optimal experimental designs. Technometrics 16, 203–210.

O'Reilly, S., Wilson, C., Hardy, J., 1987. The influence of food on the gastric emptying of multiparticulate dosage forms. Int. J. Pharm. 34, 213–216.

Prinderre, P., 2008. FR Patent no. EP 08290529.

Sangekar, S., Vadino, W.A., Chaudry, I., Parr, A., Beihn, R., Digenis, G., 1987. Evaluation of the effect of food and specific gravity of tablets on gastric retention time. Int. J. Pharm. 35, 187–197.

Scheffé, H., 1963. Simplex-centroid design for experiments with mixtures. J. R. Stat. Soc. B 25, 235–263.

Sonobe, T., Watanabe, S., 1989. JP Patent no. JP 19890225245.

Streubel, A., Siepmann, J., Bodmeier, R., 2002. Floating microparticles based on low density foam powder. Int. J. Pharm. 241, 279–292.

Streubel, A., Siepmann, J., Bodmeier, R., 2003a. Floating matrix tablets based on low density foam powder: effects of formulation and processing parameters on drug release. Eur. J. Pharm. Sci. 18, 37–45.

Streubel, A., Siepmann, J., Bodmeier, R., 2003b. Multiple unit gastroretentive drug delivery systems: a new preparation method for low density microparticles. J. Microencapsul. 20, 329–347.

Struebel, A., Siepmann, J., Bodmeier, R., 2006. Gastroretentive drug delivery systems. Expert Opin. Drug Deliv. 3, 217–233.

Talwar, N., Sen, H., Staniforth, J., 2000. WO Patent no. WO 0015198.

Timmermans, J., 1991. Floating Hydrophillic Matrix Dosage Forms for Oral use: Factors Controlling Their Buoyancy and Gastric Residence Capabilities. Ph.D. Thesis. University of Brussels, Belgium.

Timmermans, J., Moës, A., 1990a. How well do floating dosage forms float? Int. J. Pharm. 62, 207–216.

Timmermans, J., Moës, A., 1990b. Measuring the resultant-weight of an immersed test material: I. Validation of an apparatus and a method dedicated to pharmaceutical applications. Acta Pharm. Technol. 36, 171–175.

Timmermans, J., Moës, A., 1990c. Measuring the resultant-weigthof an immersed test material: II. Examples of kinetic determination applied to monolithic dosage forms. Acta Pharm. Technol. 36, 176–180.

Vanderbist, F., Baudier, P., Deboeck, A., Amighi, K., Goole, J., 2007. BE Patent no. WO 2007106960.